Adaptive Mitigation of Narrowband Interference in Impulse Radio UWB Systems Using Time-Hopping Sequence Design

Mohamed E. Khedr, Amr El-Helw, and Mohamed Hossam Afifi

Abstract: **The coexistence among different systems is a major problem in communications. Mutual interference between different systems should be analyzed and mitigated before their deployment. The paper focuses on two aspects that have an impact on the system performance. First, the coexistence analysis, i.e. evaluating the mutual interference. Second aspect is the coexistence techniques, i.e. appropriate system modifications that guarantee the simultaneous use of the spectrum by different technologies. In particular, the coexistence problem is analyzed between ultra-wide bandwidth (UWB) and narrow bandwidth (NB) systems emphasizing the role of spectrum sensing to identify and classify the NB interferers that mostly affect the performance of UWB system. A direct sequence (DS)-time hopping (TH) code design technique is used to mitigate the identified NB interference. Due to the severe effect of Narrowband Interference on UWB communications, we propose an UWB transceiver that utilizes spectrum-sensing techniques together with mitigation techniques. The proposed transceiver improves both the UWB and NB systems performance by adaptively reducing the mutual interference. Detection and avoidance method is used where spectrum is sensed every time duration to detect the NB interferer's frequency location and power avoiding it's effect by using the appropriate mitigation technique. Two scenarios are presented to identify, classify, and mitigate NB interferers.**

Index Terms: **Code sequence design, coexistence, cognitive radio (CR), impulse radio (IR), interference mitigation, matched filter (MF), narrowband (NB) interference, spectrum sensing, spectrum shaping, spread-spectrum (SS).**

I. INTRODUCTION

THE increasing demand for higher data rates in personal area networks have led to the current interest and development in yltra-wide bandwidth (UWB) communications technology. UWB is a promising candidate for high speed, low power, low complexity and extensive resources short-range indoor wireless communications [1]. Although UWB was used for positioning, military communications, radar and sensing 20 years ago, it has been focused on consumer electronics and communications only very recently. In 2002, the Federal Communications Commission (FCC) allocated a huge bandwidth of 7,500 MHz in 3.1–10.6 GHz at the noise floor, where UWB devices are allowed to operate under certain spectral masks for indoor and outdoor applications. A signal is classified as UWB if its bandwidth is larger than 500 MHz or its fractional bandwidth is larger than 20. The strength of UWB systems lies on the use of extremely wide transmission bandwidths, resulting in desirable capabilities, including accurate position location and ranging [6], lack of significant multipath fading due to fine delay resolution, multiple access (MA), high data rates and possible easier material penetration due to low-frequency components. Moreover, as a result of low transmission power operation UWB offers a covert communications. Large transmission bandwidths, on the other hand, introduce new challenges where UWB have to successfully coexist with the overlapping existing narrow bandwidth (NB) services [7], [8]. In fact, most of the wireless communication systems use separate narrowband frequencies in order to avoid interference to each other. However, in order for UWB systems to avoid interference with other NB services, they have to meet the spectral mask defined in the FCC's report [3] in February 2002, which means they emit in very low power levels. The effect of NB interference on UWB remains an important topic which is investigated in [9] and [10]. Notch filter, non-linear prediction filter, and minimum mean square-error (MMSE) rake reception where performed at the receiver as NB suppression techniques to reduce the interference effect [11]–[13]. However these techniques are used to reduce the interference on UWB signals, the interference caused by UWB signals to licensed NB signals must be efficiently mitigated. Spectrum shaping of UWB signals is an effective approach to suppress the mutual interference between UWB and NB systems, where notches are created at the frequencies dedicated to NB services. By transmitting low signal power in the overlapping bands UWB reduces the interference to NB systems. On the other hand, the matched filter (MF) receiver of UWB will act as a notch filter that removes the undesired NB interference. References [14], [15] shaped the UWB spectrum through pulse shaping. One promising and simple approach for shaping the UWB signal spectrum is by design of the direct sequence (DS) or the time hopping (TH) sequence in UWB signals [16], [17]. However they mitigated the mutual interference between NB and UWB through using one of these sequences, they lost the desired properties of spread-spectrum (SS) signals. To maintain both, mutual interference suppression and gaining SS benefits, [18] used both DS designs to minimize the interference from a single NB interferer and TH sequences to preserve the desired SS signal properties. In [19], eigenvalues and vectors were used to design DS and TH sequences by alternation for shaping UWB spectrum. Two scenarios were considered wherein the first scenario DS was used for NB interference mitigation and was able

Manuscript received June 21, 2013; approved for publication by Xiaodai Dong, Division II Editor, January 14, 2015.

Department of electronics and communications Arab Academy for Science, Technology and Maritime Transport, Alexandria, Egypt, email: Khedr@vt.edu, {elhelw, hossam.afifi}@aast.edu.

Digital object identifier 10.1109/JCN.2015.000109

to minimize multiple interferer's power, while in the second scenario where TH sequence was used for mitigation the proposed technique was able to mitigate a single NB interferer. The designed TH code in [19] can mitigate a single NB interferer, however UWB signals suffer from multiple NB interferers with varying powers, which leads to a severe performance degradation. In this study, detection and adaptive avoidance techniques are used to mitigate the interference, in order to avoid the performance decay of possible primary users, operating in the same spectrum portions as shown in Fig. 1. These techniques are mainly composed of two phases. The aim of the first phase is to perform some sort of detection and classification on the primary user. If there are one or more active primary users in some band portions, the second phase is started, which utilizes techniques able to protect the primary user's performances in those portions of the transmission resource. The UWB device will therefore have to apply periodical sensing cycles, in order to detect the activity of possible licensed systems, by working autonomously, with no cooperation from them. Spectrum sensing can be accomplished in different ways [20], [21]. Energy detector based approach is the most common way of spectrum sensing because of its low computational and implementation complexities [22]–[24]. In addition, receivers do not need any knowledge on the primary users signal. The signal is detected by comparing the output of the energy detector with a threshold, which depends on the noise floor. In selecting a sensing method, two issues should be considered. The first issue is that the spectrum is sensed to determine the interferer with highest power, i.e. power is collected without comparing to a threshold. The second issue is that a simple UWB transceiver is built, i.e. seeking a sensing method that reduces the added complexity should be done. As a consequence, energy detector (ED)'s are embedded in the classifiers. In this paper, two scenarios with two case studies are introduced. In the first scenario, the frequency locations of the NB interferers are previously known and spectrum sensing will take place to detect the interferer with highest average power where TH code design is used to mitigate the effect of the interferer. In the second scenario, frequency locations of NB interferers are unknown and linear spectrum sweeping is done to detect the interferer with the highest average power all over the BW dedicated for UWB where mitigation is done through TH code design. The rest of this paper is organized as follows. The UWB system structure and model, including transmitter, NB interference, channel response, and receiver are described in Section II. The proposed UWB transceiver is suggested in Section III. Section IV discusses the NB interference identification and classification in UWB systems through energy detection spectrum sensing. The algorithm of TH code design for NB interference mitigation is then discussed in Section V. The proposed transceiver's performance under practical considerations is then studied in Section VI. Section VII gives representative simulation results of system performance under various conditions. Finally, Section VIII draws the conclusions.

II. UWB STRUCTURE AND MODEL

We consider a binary communication system with MF reception. The transmitter in Fig. 2. generates a DS-TH UWB signal,

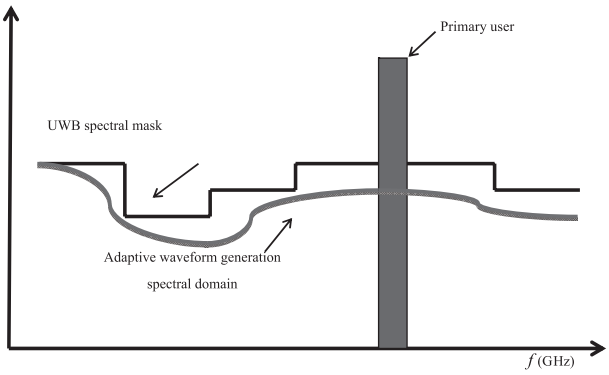

Fig. 1. Adaptive avoidance of narrowband interference from primary users.

which can be represented by the following model,

$$S_u(t) = \sqrt{E_u} \sum_i (b(t - iT_b; d_i),\ d_i \in \{0, 1\} \tag{1}$$

where

$$b(t; d_i) = (2d_i - 1) \sum_{k=0}^{N_s - 1} C_k^{\mathrm{DS}} p(t - kT_f - C_k^{\mathrm{TH}} T_c) \tag{2}$$

is a unit-energy waveform used to transmit a single information bit d_i, belonging to the set $\{-1, 1\}$. E_u the energy per transmitted bit, $T_b = 1/R_b$ is the bit duration, N_s is the number of pulses. The pulse repetition time (frame length) T_f and the bit duration T_b are related by $T_b = N_s T_f$. Finally C_k^{TH} is the TH sequence, $T_c$is the TH chip width, and C_k^{DS} is the DS spreading sequence. The bit waveform (2) is valid for a general transmitted scheme that combines TH and DS, and results in pure TH when $C_k^{\mathrm{DS}} = 1,\ \forall\, k$, and pure DS when $C_k^{\mathrm{DS}} = 0,\ \forall\, k$.

In this study, as shown in Fig. 3, a combination of TH and DS is used where TH code is used for multiple access (MA), DS code for NB interference mitigation and vice-versa. NB interference can be modeled as in [9] and [10].

$$S_n(t) = \sqrt{2I_n} \cos(2\pi f_n t + \vartheta_n) \tag{3}$$

While UWB signals cover a large bandwidth it is reasonable to assume that they experience a frequency-selective fading channel with channel impulse response [25],

$$h_u(t) = \sum_{l=0}^{L-1} h_{u,l}\, \delta(t - \tau_{u,l}). \tag{4}$$

NB signals, which have a small bandwidth, experience a frequency-flat fading channel with impulse response

$$h_n(t) = \alpha_n \delta(t - \tau_n). \tag{5}$$

The received signal at UWB single branch receiver can be expressed as in [9]

$$r(t) = \sqrt{E_u} \sum_i r_u(t - iT_b; d_i) + \sum_{n=1}^{N_n} \sqrt{I_n} r_n(t). \tag{6}$$

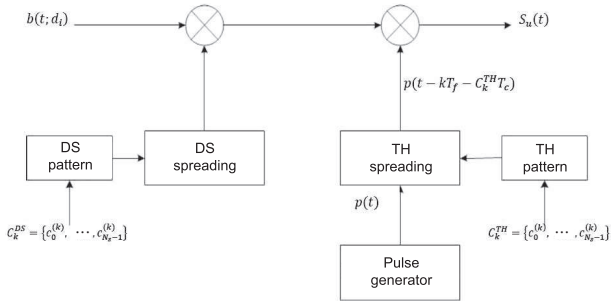

Fig. 2. The UWB direct sequence time hopping transmitter.

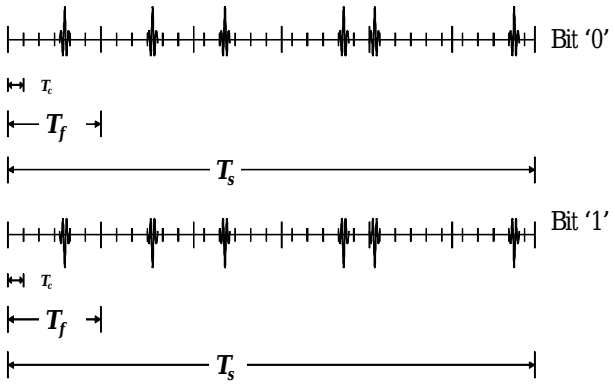

Fig. 3. Transmitted DS-TH UWB signal at $N_s = 6$ and $N_h = 6$.

where $r_u(t;d_i) = b_u(t;d_i) \otimes h_u(t) = \sum_{l=0}^{L-1} h_{u,l} b(t-\tau_{u,l}\,;d_i)$ is the received waveform of the ith UWB information bit, $r_n(t) = s_n(t) \otimes h_n(t) = a_n s_n(t-\tau_n)$ is the interfering signal from the nth NB user, n(t) is additive white Gaussian noise with double-sided PSD of $N_{0/2}$. The received signal in (6) is affected by AWGN and interference. If only AWGN is present, the optimum receiver consists of a filter, matched to the difference $r_u(t;0) - r_u(t;1)$ or, equivalently, a correlator followed by a sampler. The template waveform of the correlator v(t) is given by

$$v(t) = r_u(t;0) - r_u(t;1). \tag{7}$$

Assuming perfect synchronization with the desired signal, the MF output u(t) at the appropriate sampling instant t_0 is

$$u(t_0) = s_0 + \sum_{n=1}^{N_n} \alpha_n \sqrt{2I_n}\,|H(f_n)| \cos(\phi_n) + n_0 \tag{8}$$

where s_0 is the desired signal

$$s_0 = \sqrt{E_b} \int_{-\infty}^{t_0} r_u(t;d_0) v(t) dt. \tag{9}$$

$H(f)$ is the MF transfer function and n_0 is the noise sample with zero mean and variance $\sigma^2 = (N_0/2)\int_{-\infty}^{\infty} v(t)^2 dt$. The MF is matched to the received waveform, so its transfer function can be easily evaluated as

$$H(f) = F(v(t)) = F(r_u(t;0) - r_u(t;1)) \tag{10}$$

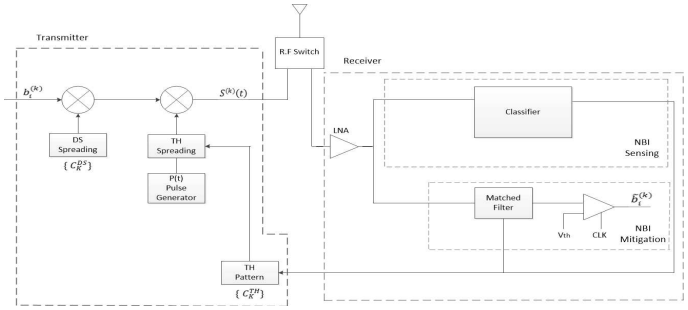

Fig. 4. The adaptive mitigation UWB transceiver.

where $F\{.\}$ denotes the Fourier transform. Since $H(f)$ can be written as

$$H(f) = |H_0(f)|\,|F(h_u(t))| \tag{11}$$

where

$$H_0(f) = F\{b(t;0) - b(t;1)\}; \tag{12}$$

$$|H_0(f)| = 2\,|p(f)| \left| \sum_{k=0}^{N_s-1} C_k^{\mathrm{DS}} e^{j2\pi f(kT_f + C_k^{\mathrm{TH}} T_c)} \right|. \tag{13}$$

Since we assume that NB signals propagate through Rayleigh fading channels and the phase distortion in (8) is uniformly distributed in [0, 2π], the interference term in (8), which includes NB interference and AWGN, is Gaussian distributed conditioned on the channel impulse response (CIR). Therefore, the bit error rate (BER) of the Rake receiver conditioned on the CIR is given as $P_{(e/h,t)} = Q\left(\sqrt{2\mathrm{SINR}_{\mathrm{con}}}\right)$, and $\mathrm{SINR}_{\mathrm{con}}$ is the signal-to-interference-plus-noise ratio (SINR) conditioned on the UWB CIR. This conditional SINR can be expressed [5].

$$SINR_{C,O,N} = \frac{S(h)}{\frac{N_0}{E_u} + \sum_{n=1}^{N_n} \frac{I_n |H_0(f)|^2 |H_u(f_n;h,t)|^2}{C T_b S(h)}} \tag{14}$$

where $C = E_b/T_b$ and $s(h) = \sum_{l=0}^{L-1} h_{u,l}^2$.

III. THE PROPOSED UWB TRANSCEIVER

Assuming that the transmitter and receiver are within a coherent distance, i.e. they are experiencing the same NB interference effect. As stated in [19], the designed TH code can only cope with the mitigation of a single NB interferer. However UWB signals suffer from multiple NB interferers with varying powers, which lead to a severe performance degradation. To adapt with this frequency location variation, a transceiver with spectrum sensing ability is proposed. Therefore the classifiers presented in Section IV are added to the transceiver structure. In the first scenario, the frequency locations of the NB interferers are previously known and spectrum sensing will take place to detect the interferer with highest average power where TH code design is used to mitigate the effect of the interferer.

As shown in Fig. 4 the proposed transceiver improves the performance of the system by using the first classifier in Section IV for sensing the spectrum every certain duration. A group of tuned BPF's is used over the bandwidth of the previously known

interferers frequency locations. The output signal is mixed with frequencies generated from the local oscillators (LO) adjusted at the known NB locations passing by an integrator to generate a decision metric for each interferer. Processing is done to identify the interferer with the highest power. The frequency location of this NB interferer is then an input to the TH code design algorithm discussed in Section V. The designed TH code shapes the spectrum of the transmitted waveform and in turn shapes the transfer function of the MF creating notch at this frequency location. The proposed transceiver with the utilization of this classifier has a relatively simple structure however this is not the common scenario as the interferers frequency locations are not commonly previously known. Moreover the bandwidth dedicated to every NB interferer isn't also known. As a consequence another transceiver is proposed for a different case scenario. In the second scenario, frequency locations of NB interferers are unknown. Linear spectrum sweeping is done to detect the interferer with the highest average power allover the BW dedicated for UWB where mitigation is done through TH code design.

On the other hand the proposed transceiver receiver in Fig. 4, which uses the second classifier in Section IV, scans the whole UWB dedicated spectrum to detect the frequency location of the highest NB interferer. A group of BPF's is used to divide the total spectrum into N bands. The output of each BPF is then mixed with N frequencies generated from the N local oscillators (LO). Fast Fourier transform (FFT) is then used as each band is divided into small parts. Each M-parts correspond to a certain NB interferer. Determining the mth part with highest average power using energy detection will enable determining the frequency location of the NB interferer to be mitigated using TH code design algorithm discussed in the previous section. The proposed transceiver adds more complexity to the design however it improves the UWB system SNR enabling it to mitigate the NB interference effect. It is important to notice here that since the transmitter and the receiver are assumed to be experiencing the same NB interferer's effect, therefore the same TH code designed at the transmitter will be generated at the receiver.

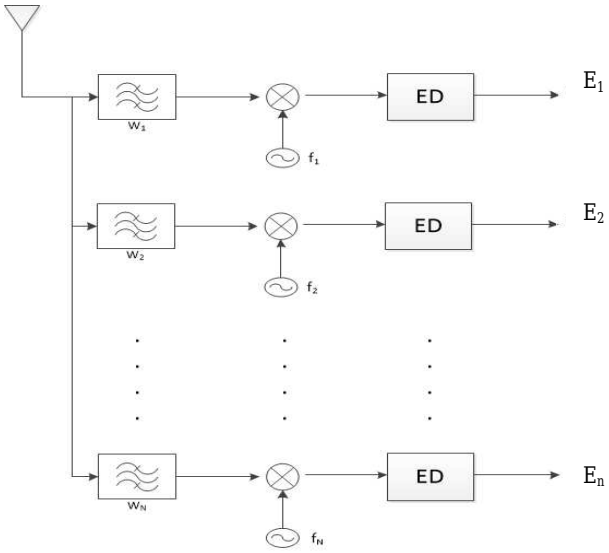

Fig. 5. Narrowband interferer's classifier.

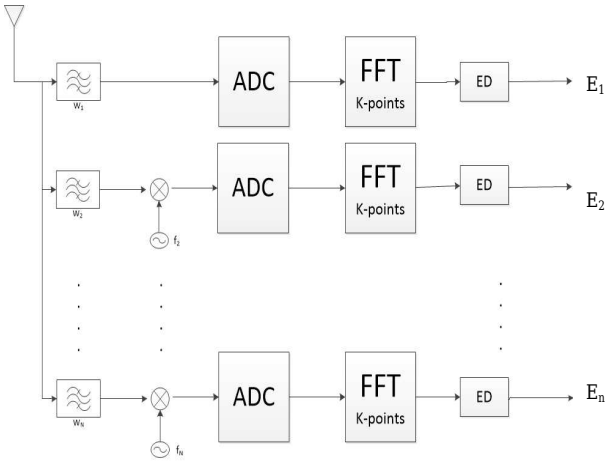

Fig. 6. Narrowband interferer's location identifier and classifier.

IV. PROPOSED NB INTERFERENCE CLASSIFIERS

Spectrum sensing for UWB communications have different requirements when compared to the narrowband based cognitive radios. The key difference here is the larger portion of the spectrum to be scanned in real time for the UWB systems compared to the narrowband systems. The classifier in Fig. 5 senses the UWB spectrum (B) at previously known frequency locations where N primary users exist. The nth BPF tuned at the center frequency fn of nth primary user with bandwidth W_n chosen according to the technology. The output of the BPF is then down-converted and the energy detector (ED) [26] is used to generate the decision statistic E_n, which is a measure of the power of the nth interferer. Output of the classifier is the vector E;

$$E = [E_1\ E_2 \cdots E_n] \tag{15}$$

corresponding to the primary users operating at frequency locations of vector f;

$$F = [f_1\ f_2 \cdots f_n]. \tag{16}$$

The frequency location of this NB interferer is then an input to the TH code design algorithm discussed in the next section. The designed TH code shapes the spectrum of the transmitted waveform and in turn shapes the transfer function of the MF creating notch at this frequency location. In the classifier in Fig. 6, NB interferers frequency locations are assumed to be unknown so the classifier has to sense the whole UWB spectrum (B) to identify the presense of each interferer and it's location. Instead of sensing the whole spectrum which needs a very high sampling frequency (f_s), as the UWB spectrum is around 7.5 GHz, the proposed classifier divides the total UWB sensed spectrum into N bands using N BPF's. Bandwidth of all BPF's is constant and can be calculated as $W = B/N$.

The spectrum of each branch is spanned using FFT. The FFT block has (K) outputs with a frequency span of ($\triangle f$), for a W total bandwidth. For a decision to be taken the classifier needs (b) bins of the total K points i.e., the output of each detector is a vector E of length $M = K/b$, where b is number of bins per $\triangle f$ and $\triangle f = W/M$. Decisions of each detector can be collected

in a vector E, which describes the status of the PU's spectrum usage over the band W, $E = [E_1 E_2 \cdots E_M]$corresponding to the primary users operating at frequency locations of vector f $f = [f_1 f_2 \cdots f_M]$. In (17) and (18) each element of the generated $N \times M$ matrix corresponds to a NB interferer location and power measure respectively

$$f_{n,m} = \begin{bmatrix} f_{1,1} & \cdots & f_{1,m} \\ f_{2,1} & \cdots & f_{2,m} \\ f_{n,1} & \cdots & f_{n,m} \end{bmatrix}, \tag{17}$$

$$E_{n,m} = \begin{bmatrix} E_{1,1} & \cdots & E_{1,m} \\ E_{2,1} & \cdots & E_{2,m} \\ E_{n,1} & \cdots & E_{n,m} \end{bmatrix}. \tag{18}$$

To identify, the interferer with the highest power, the decision matrix E must be analyzed. The location of the highest element in matrix E corresponds to the frequency location of the highest interferer in matrix f. The proposed classifier in Fig. 5 enhances the sensing performance by decreasing both the sensing time, and the burden on the ADC by minimizing the needed sampling frequency by an order N. However it adds complexity to the transceiver's structure by adding N branches.

V. TH CODE DESIGN FOR NB INTERFERENCE MITIGATION

In this section, a pseudonoise (PN) code is used as the direct sequence code for the desired UWB. This PN sequence is known by the UWB device where a TH sequence design will be proposed based on the DS and the spectrum occupation information in the UWB victim link. The TH code is designed as to minimize the response of the matched filter at frequency locations of NB interferers. As derived in [9] conditional SINR recall (14), conditioned on the CIR, is expressed as

$$\mathrm{SINR}_{CO,N} = \frac{S(h)}{\frac{N_0}{E_u} + \sum_{n=1}^{N_n} \frac{I_n |H_0(f)|^2 |H_u(f_n;h,t)|^2}{C T_b S(h)}}. \tag{19}$$

It is important to notice that $H(f)$ is composed of two factors, the first depends on the waveforms used, while the second depends on the CIR for the desired signal. Therefore to minimize the mutual interference effect we can only control the first term. Maximizing the conditional SINR is equivalent to minimizing the interference term in (19) which is

$$\sum_{n=1}^{N_n} I_n \left|H_0(f)\right|^2. \tag{20}$$

Recall that $H_0(f)$ depends on the waveforms used where,

$$\left|H_0(f)\right| = 2\left|p(f)\right| \left| \sum_{k=0}^{N_s-1} C_k^{\mathrm{DS}} e^{j2\pi f (kT_f + C_k^{\mathrm{TH}} T_c)} \right|. \tag{21}$$

Spectrum is shaped by designing the appropriate TH code used in the formation of UWB waveforms to create notches at the frequency locations of NB interferers. Hence, the TH sequence designs also reduce the power transmitted by UWB signals at the dedicated NB locations, and the interference caused by UWB devices to NB services is subsequently reduced. It should be noticed here that the response of the MF is identical to the spectrum of the transmitted signal [25]. According to [19] the proposed algorithm can only cop with a single NB interferer, i.e., the objective function is to minimize $H_0(f)$ at a single frequency location f_1. Which is the frequency location determined from the sensing phase described in the previous section.

$$\left|H_0(f)\right|^2 = \left| \sum_{k=0}^{N_s-1} e^{j2\pi f_1 C_k^{\mathrm{TH}} T_c} C_k^{\mathrm{DS}} e^{j2\pi f_1 T_f} \right|^2 \tag{22}$$

which can be written in the form

$$\left|H_0(f)\right|^2 = C_{\mathrm{TH},e}^* \left(V_{p,1} V_{p,1}^*\right) C_{\mathrm{TH},e} = C_{\mathrm{TH},e}^* Q_{\mathrm{TH}} C_{\mathrm{TH},e} \tag{23}$$

where

$$\begin{aligned} Q_{\mathrm{TH}} &= (V_{p,1} V_{p,1}^*); \\ V_{p,1} &= (P_{0,1}, \cdots, P_{N_s-1,1}); \\ p_{k,1} &= c_k^{\mathrm{DS}} \exp(j2\pi f_1 k T_f); \\ C_{\mathrm{TH},e} &= (c_0^{\mathrm{TH},e}, \cdots, c_{N_s-1}^{\mathrm{TH},e}); \\ c_k^{\mathrm{TH},e} &= \exp(j2\pi f_1 c_k^{\mathrm{TH}} T_c). \end{aligned}$$

The design procedure can be summarized as follows [19]: Time-hopping sequence design algorithm.

1) Find the smallest eigenvalue of $Q_{\mathrm{TH}} = V_{p,1} V_{p,1}^*$ and the corresponding eigenvectors $q_1, \cdots, q_m$ where $m \geqslant 1$.

2) If any of the eigenvector is in $I_{\mathrm{TH}}^{N_s}$, i.e., all the components of the vector belong to the set $\mathrm{D} = \{d_0, \cdots, d_{N_{h-1}}\}$, the search is over and $C_{\mathrm{TH},e}$ is set to be this eigenvector.

3) If the condition in Step 2 fails, for each eigenvector q_i find a sequence $\tilde{q}_i = Int_{\mathrm{TH,app}}(q_i)$ where $Int_{\mathrm{TH,app}}(V)$ is given by $\tilde{v} = Int_{\mathrm{TH,app}}(V)$, where $\tilde{v}_j = d_k = \exp(j2\pi f_1 k T_c)$

$$k = \operatorname{argmin} \left|\mathrm{Arg}(v_j - d_k)\right| \tag{24}$$

where the distance between q_i and $\tilde{q}_i$ is given by

$$D(q_i, \tilde{q}_i) = \sqrt{\sum_{j=0}^{N_s-1} (q_{ij} - \tilde{q}_{ij})^2}. \tag{25}$$

4) Find the TH sequence C_{TH} based on $C_{\mathrm{TH},e}$ according to their relationship, i.e., if the lth component of $C_{\mathrm{TH},e}$, $c_l^{\mathrm{TH},e} = \exp(j2\pi f_1 c_l^{\mathrm{TH}} T_c) = d_k$, the lth component of the TH sequence, $c_l^{\mathrm{TH}} = k$. A numerical example is solved in Appendix clarifying the steps used to reach the suitable TH code design forming notch at the specified frequency location at $N_s = 3$ and $N_h = 3$.

VI. PERFORMANCE CONSIDERATIONS

Energy detector based approaches are the most common way of spectrum sensing because of their low computational complexity. Moreover, they are more generic as the receiver does not need any knowledge on the primary users signal. The main dilemma for any device combining communication and sensing

is the issue of resource allocation to each task. The most important resource is time. It is impractical to sense the environment while transmitting given the cost complexity limitations. Obviously, the consequence of allocating dedicated sensing time is lower communication throughput. If a device sensed the environment for 50% of the time, the throughput of the devices in its network would decreased by at least those same 50. The problem statement and the formulation presented here, is provided in [27], [29] in more details. The transceiver is assumed to sweep the UWB frequency (3.1–10 GHz) linearly in time and cyclically with a single scanning duration of Tw seconds. We define the term linear-sweeping where the sensing node sweeps the spectrum linearly with time, and cyclic-sweeping where the sensor node starts back to sweep from 3.1 GHz up to 10 GHz after completing the previous cycle for the same frequency range.

Given a legacy user in the UWB frequency band with a bandwidth of BW (Hz), and its corresponding temporal characteristics for the occupancy and the idle durations as τ and Δ respectively following some arbitrary distributions, the cognitive radio node will detect the presence of the legacy user only during the time period of t_{1m} to t_{2m} which corresponds to the time period in scanning the frequencies from f_1 to f_2 during its mth scan. Fig. 7 depicts the frequency sweeping process of the cognitive radio and the transmission patterns of the legacy user in time. In this figure, the triangular curves show the frequency scanning process from 3.1 GHz to 10 GHz with respect to the time scale, and the horizontal bar represents the transmission pattern of the legacy user between f_1 and f_2 with respect to the time scale. As shown in Fig. 7, the sensor node only scans the frequencies from f_1 to f_2 when the horizontal bar intersects with the triangular curve, i.e. the intersection in time between the scanning process and the legacy user transmission, which corresponds to the timing period of t_{1m} to t_{2m} for the mth scan. The transceiver on the other hand will only detect the legacy user when the legacy user is transmitting within this time period and any other transmissions from the legacy user outside this time period is gone undetected. When scanning a wide range of frequencies (7.5 GHz), a narrow band PU, which has a bandwidth much smaller than the UWB user, can be gone undetected. It is obvious to state that such miss detection depends on the PU 's transmission statistics, or in other words the spectral occupancy statistics (SoS) and the corresponding time required to sense the spectrum. As it scans a spectrum of W in a duration Tw, the classifier scans the entire spectrum linearly at a rate of W/T_w. Using such a linear frequency sweeping process, given that the PU is transmitting, the classifier can only detect the PU during its mth scan within the time slot only from $t_1^m = t_o + f_1 T_w/W + (m-1)T_w$ and $t_2^m = t_o + f_2 T_w/W + (m-1)T_w$, where t_o is an arbitrary real constant, f_1 and f_2 are the edge frequencies of the transmission bandwidth of the PU with $m = 1, 2, \cdots$, and $f_1 < f_2$. Initially, the transmission duration (hold time) τ of the PU is assumed to be a constant to simplify the analysis. In order to perform theoretical analysis some mathematical model should be followed for the temporal characteristics of the PU. The Poisson model for the arrival process is the most common model used in the research literature for theoretical derivations and performance analysis, therefore such a model is adopted in the work. As the PU's transmission, is modeled as a Poisson arrival process, therefore Δ follows an exponential distribution [28] with a mean time between transmission given by Δa. To define the primary user's spectral occupancy statistics based on the Poisson arrival process we consider some axioms. It is important to note that these axioms are the fundamentals in defining the Poisson arrival process in general, and based on these axioms the spectrum sensing detection performances considering the spectral occupancy model of the PU is then analyzed.

Let $N(t)$ be the number of times that the PU has been present in the spectrum (number of transmissions) up to time t [29].

Axiom 1: At time $t = 0$ the PU has got no occupancy of the spectrum. That is, $N(0) = 0$.

Axiom 2: Incremental independency and stationarity of $N(t)$. That is, if $J_1 = N(t_2) - N(t_1)$ and $J_2 = N(t_4) - N(t_3)$ for some $t_1; t_2; t_3; t_4$ such that $t_1 < t_2 < t_3 < t_4$, then J_1 and J_2 are independent. Further, if $t_4 - t_3 = t_2 - t_1$, then J_1 and J_2 have the same statistical distributions. The Poisson distribution for the arrival process is then given by,

$$P[N(t) = n] = e^{-\lambda t}\frac{(\lambda t)^n}{n!} \tag{26}$$

where, $n = 0, 1, 2, \cdots$, and $\lambda = 1/\Delta a$ is the mean arrival (spectral occupancy) rate of the PU. On the other hand, the occupancy time τ of the PU is initially considered to be a constant. The detection performance of the classifier is characterized by the SoS of the PU, the bandwidth BW of the PU, and the total time T_w for the classifier to scan the entire bandwidth W. Occupancy probability: For the PU, we define the spectral occupancy probability P_0 as the probability of starting at least one transmission by the PU over a time of T_0 seconds. Therefore P_0 is given by $P_0 = P[N(t = t_0) \geqslant 1, \forall t_0 > 0]$. From (26) we find a closed form expression for the probability of occupancy as,

$$P_0 = 1 - e^{(-\lambda t_0)}. \tag{27}$$

From (27), we can compute the spectral occupancy probability of the PU for a single scanning period T_w by letting $T_0 = T_w$. $P_0 = 1 - \exp(-\lambda t_w)$. It should be noticed here that Po depends mainly on two parameters λ and T_w .

The first parameter is related to the PU's action where, as the arrival rate increases the P_0 will increase. The second parameter is related to the classifier, as any increase in the sensing time leads to higher P_0.

Detection probability: The detection probability, for detecting the PU by the classifier over a single scan duration of T_w, is defined by the probability of starting at least one transmission within the time slot of $t_1^m - \tau < t < t_2^m$ for the mth scanning iteration. The probability of detection is given by $P_d = P[N(t_2^m) - N(t_1^m - \tau) \geqslant 1]$. Using the incremental independence and stationarity property of the arrival process (Axiom 2), P_d can be rewritten as $P_d = P[N(\tau + \Gamma) \geqslant 1]$, where $\Gamma = t_2^m - t_1^m = (T_w(f_2 - f_1))/W$ and from (26) we find a closed form expression given by,

$$P_d = 1 - e^{-\lambda(\tau+\Gamma)} \tag{28}$$

Note that when $\tau + \Gamma = T_w$ then $P_d = P_0$, therefore the classifier detects all the transmissions from the PU in a single scanning period. At the same time we also observe from (28) that

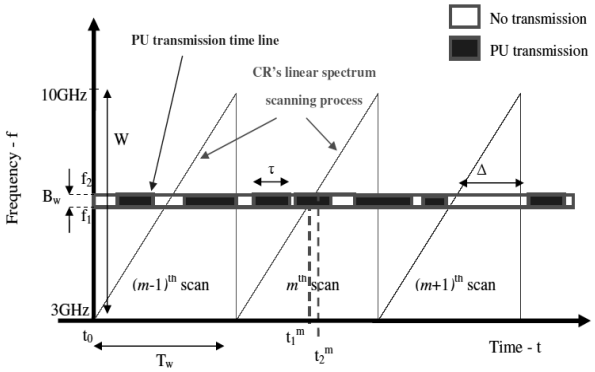

Fig. 7. Linear sweeping of the UWB spectrum and the temporal characteristics of the legacy user transmission [29].

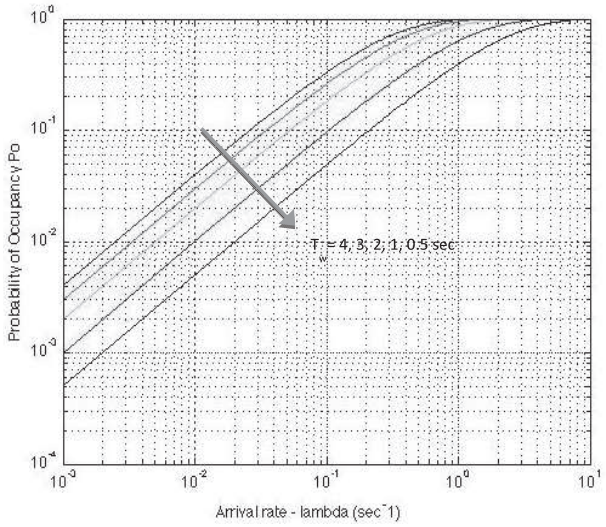

Fig. 8. Probability of occupancy at different scanning durations.

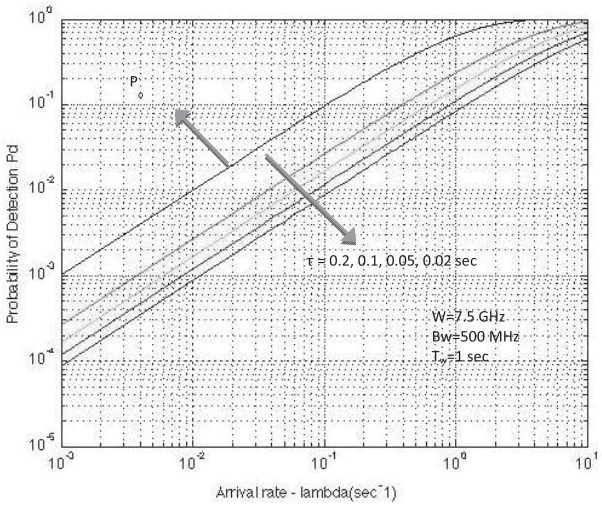

Fig. 9. Probability of detection at different hold times.

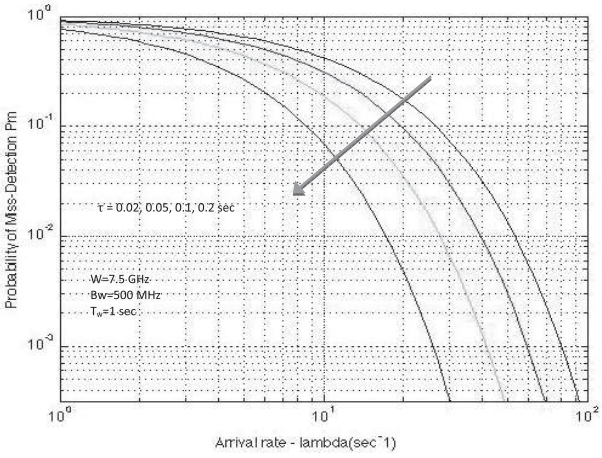

Fig. 10. Probability of miss detection at different hold times.

$P_d = 1$ when $\lambda \to \infty$. It is important to realize that as Γ increases P_d increases. The increase in Γ may be a reason of an increase in T_w, or in Bw i.e., $f_2 - f_1$, while an increase in the total sensed spectrum W will logically lead to a decrease in the P_d.

Miss detection probability: The probability of miss detection occurs when there is at least one initiation of transmission occurring for some t outside the interval $t \notin [t_1^m - \tau, t_2^m]$, but no initiations (of transmissions) during the interval, in a single scan, and since $P_d = 1 - P_M$ then $P_m = \exp(-\lambda(\tau + \Gamma))$. Fig. 8 presents the occupancy probability P_0 for various time durations To. It could be observed that P_0 increases with the arrival rate λ, as expected, and also marginally improves with the time duration T_0. The figure shows how the spectral occupancy probability of the PU (defined over a period of $T_0 = T_w$) increases when the scanning duration T_w increases for a given arrival rate. This observation is quite important, especially while studying the minimum time requirement (minimum T_w) for sensing the PU.

Figs. 9 and 10 depict the detection probability P_d and miss detection probability PM for various holding times τ and arrival rate λ. From the figures it could be noticed that the detection performance at the classifier improves when both τ and $\lambda\hat{\mathbf{A}}$, increase, we further observe that the improvement in the detection performance is greater when λ increases than when τ increases, relatively. In Fig. 11, the effect of increasing the PU's bandwidth Bw is demonstrated. It is reasonable that as the PU's bandwidth increases the ability of the classifier to detect its location increases. As the NB interferer's bandwidth is varied from 500 to 5 MHz the P_d, at arrival rate $\lambda = 10$ vary from 0.9 to 0.7.

In Fig. 12 the effect of increasing the UWB dedicated bandwidth W is demonstrated. It is reasonable that as the UWB bandwidth increases the ability of the classifier to identify the presence of a NB interferer and detect its location decreases. As the UWB bandwidth is varied from 7.5 to 0.5 GHz the P_d, at arrival rate $\lambda = 10$ vary from, 0.7 to 0.9. A device embedded with the proposed transceiver model should provide a certain probability of detection P_d of PU at a certain arrival rate λ. In the simulations presented in Section VII PU's are assumed to have a high arrival rate λ together with a high hold time τ for each user, which provides a very high P_d guaranteeing that the primary user will always be detected, i.e., the efficiency of the proposed model is tested without considering the primary

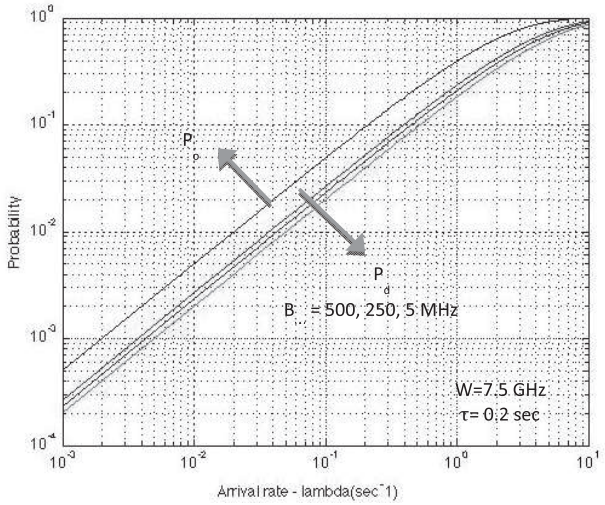

Fig. 11. Probability of detection at different scanned PU's bandwidths.

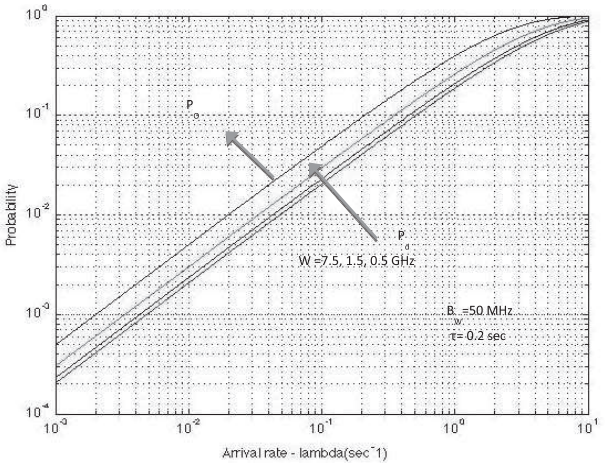

Fig. 12. Probability of detection at different scanned spectrum portions.

user behavior. Unfortunately, an increased sensing time is not the only disadvantage of the energy detector. More importantly, there is a minimum SNR below which signal cannot be detected. This minimum SNR level is referred to SNRwall [30]. In order to understand when the detection becomes impossible revisiting the signal model is needed. There, a very strong assumption is made (that is typically made in communications system analysis). Noise is assumed to be white, additive and Gaussian, with zero mean and known variance. However, noise is an aggregation of various sources including not only thermal noise at the receiver and underlined circuits, but also interference due to nearby unintended emissions.

VII. SIMULATION RESULTS

In this section, simulation results are shown to illustrate the effectiveness of the proposed adaptive NB interference mitigation transceiver structure. In the first section, the ability of different TH codes to mitigate the effect of NB interference is shown. Moreover, in the second section, the effectiveness of the proposed model is measured by comparing BER performance

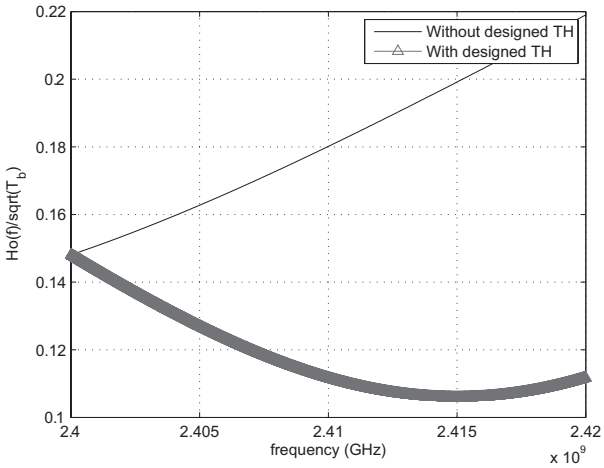

Fig. 13. Normalized transfer function of the matched filter with and without the TH code design in the presence of NB interferer at $f_n = 2.412$ GHz at $N_s = 3$.

under different scenarios. Considering the second derivative of a Gaussian monocycle with pulse duration normalization factor $\tau_p = 0.5$ ns and energy $1/\sqrt{N_s}$ given by

$$p(t) = \sqrt{\frac{8}{3N_s\tau_p}}\left[1 - 4\pi\left(\frac{t}{\tau_p}\right)^2\right] e^{\left(-2\pi\left(\frac{t}{\tau_p}\right)^2\right)}. \qquad (29)$$

Simulation parameters are given in Table 1. Pseudo random DS codes are used for multiple-access, which are randomly chosen and assumed to be known by the UWB device wherein the TH sequence design is implemented

Table 1. Simulation parameters.

Parameter	Value
N_h	3,8,16,32
N_s	3,8,16,32
τ_p	0.5 ns
T_c	1 ns
T_f	$T_c N_h$
T_b	$N_s T_f$

The role of TH code design technique to mitigate interference is first illustrated where in Figs. 13–16 the normalized transfer function of the matched filter is shown to have a notch at the frequency location of the NB interferer which was assumed to be $f_n = 2.412$ GHz at TH-DS code lengths of 3, 8, 16, and 32 respectively, therefore, the mutual interference between UWB and NB systems can be highly reduced when the designed TH sequence is applied to UWB signals.

Under the simulation parameters shown in Table 1, for measuring the effectiveness of the proposed transceiver model, BER is calculated at different scenarios. Figs. 17–19 show at $N_s = 3$, $N_s = 8$, and $N_s = 16$ comparison between BER performance of three scenarios assuming the presence of three NB interferers at $f_1 = 2.402$ GHz, $f_2 = 2.412$ GHz, and $f_3 = 2.422$ GHz and additive white Gaussian. Each figure involves three scenarios. The first scenario assumes the presence of three NB interferers

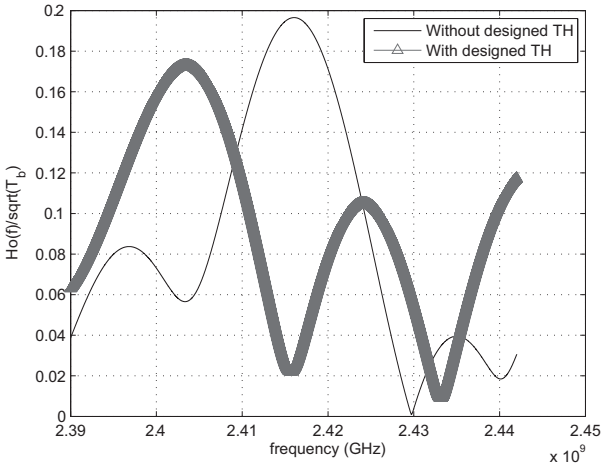

Fig. 14. Normalized transfer function of the matched filter with and without the TH code design in the presence of NB interferer at $f_n = 2.412$ GHz at $N_s = 8$.

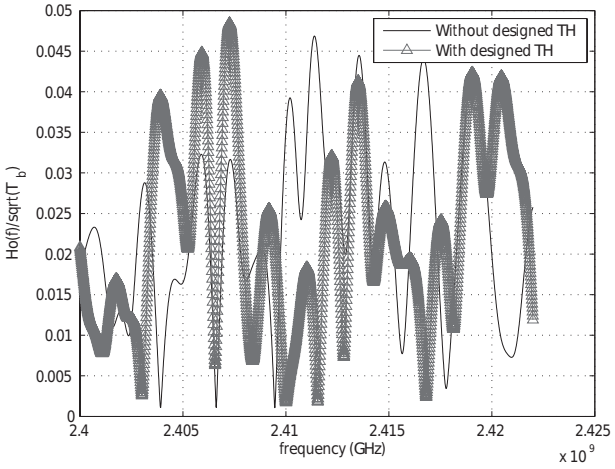

Fig. 16. Normalized transfer function of the matched filter with and without the TH code design in the presence of NB interferer at $f_n = 2.412$ GHz at $N_s = 32$.

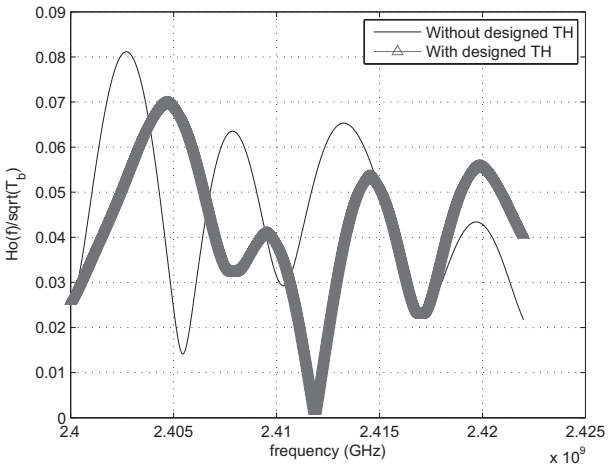

Fig. 15. Normalized transfer function of the matched filter with and without the TH code design in the presence of NB interferer at $f_n = 2.412$ GHz at $N_s = 16$.

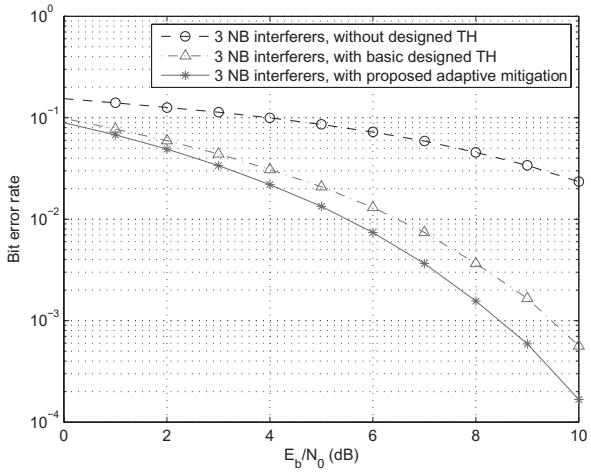

Fig. 17. Normalized transfer function of the matched filter with and without the TH code design in the presence of NB interferer at $f_n = 2.412$ GHz at $N_s = 3$

with time-varying amplitudes at frequencies $f_1 = 2.402$ GHz, $f_2 = 2.412$ GHz, and $f_3 = 2.422$ GHz where no mitigation is applied. In the second scenario the mitigation is done on a randomly selected NB interferer showing relative performance degradation due to the varying amplitudes of the interferers. The third scenario applies the proposed adaptive mitigation algorithm and shows a performance improvement than the second scenario. Note that, in the three scenarios SIR was set to be -10 dB.

In Fig. 20 spectrum is sensed every L-symbol-duration, i.e., every $L * 256$ ns, to determine the interferer with highest power and works on mitigation it's effect. The 3-D plot of time vs. frequency vs. normalized MF transfer function shows the adaptive multi-NB interferences mitigation over 8 UWB transmitted symbols where $L = 1$.

As it is stated that the sensing frequency directly affects the transceiver performance, to illustrate this idea, a random sensing time T_{sense} is chosen, i.e., spectrum is sensed every T_{sense}. To notice the effect of increasing the sensing time, a BER comparison between sensing the spectrum at T_{sense} and 2 T_{sense} is presented. The performance comparison is demonstrated at $N_s = 3$ and $N_s = 8$ in Figs. 21 and 22, respectively.

VIII. CONCLUSION

UWB technology has many attractive benefits including the extremely high wireless data transmission rate supplied by the large bandwidth covered by its signals. Deployment of such technology should guarantee the safety of overlapping technologies from a side and its own safety from the other side. In this paper, mutual interference between UWB and NB systems was investigated. DS-TH code designs were used to mitigate the mutual interference enabling successful coexistence between both

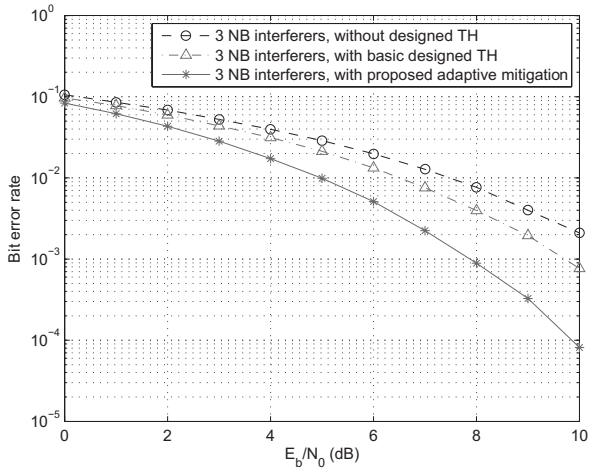

Fig. 18. Normalized transfer function of the matched filter with and without the TH code design in the presence of NB interferer at $f_n = 2.412$ GHz at $N_s = 8$.

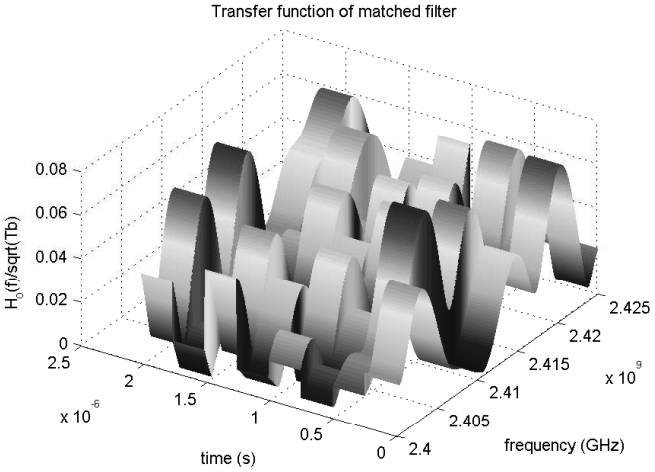

Fig. 20. Normalized transfer function of the matched filter with and without the TH code design in the presence of NB interferer at $f_n = 2.412$ GHz at $N_s = 32$.

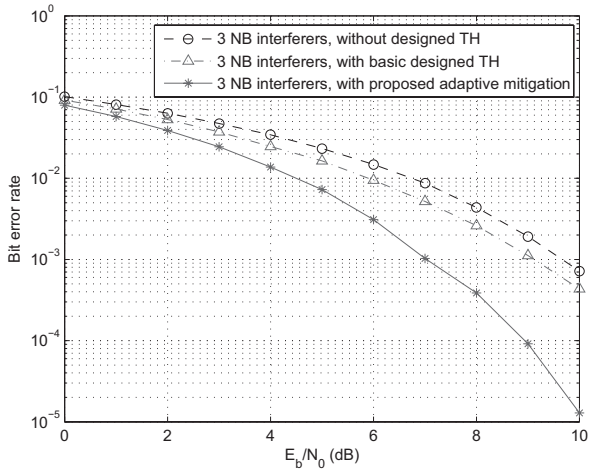

Fig. 19. Normalized transfer function of the matched filter with and without the TH code design in the presence of NB interferer at $f_n = 2.412$ GHz at $N_s = 16$.

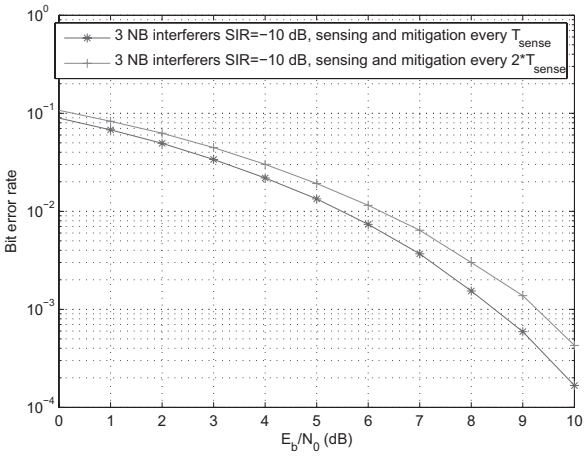

Fig. 21. Normalized transfer function of the matched filter with and without the TH code design in the presence of NB interferer at $f_n = 2.412$ GHz at $N_s = 16$.

services. However the TH code design can mitigate a single NB interferer, UWB signals suffer from multiple NB interferers with varying powers, which lead to a severe performance degradation. Spectrum sensing was used at every symbol-duration to determine and classify the NB interferer with highest power. TH spreading sequence is then designed to adaptively mitigate the effect of the identified NB interference. The proposed transceiver model is studied stating the factors affecting it's performance. Simulation results are presented to evaluate the performance of the transceiver, where they show that the proposed adaptive mitigation technique outperforms the mentioned techniques and is able to almost suppress the mutual interference effect. Simulation results showed an improvement in the proposed transceiver BER performance as the code length is increased from 3 to 8 to 16 respectively. This was well demonstrated in the BER calculations where as the code length is increased, the resolution of the designed sequence is increased, i.e. its ability to accurately mitigate the NB interference is increased. It could be observed that at BER of 0.001 our proposed model outperforms the basic mitigation model by around 1 dB, 1.8 dB, and 2.4 dB at $N_s = 3, N_s = 8$, and $N_s = 16$, respectively. The effectiveness of the proposed transceiver design should be observed as the BER performances of the proposed adaptive mitigation technique are typical to the curve of an UWB system operating in a medium with only AWGN, i.e., the effect of NB interference was perfectly mitigated. The effect of different sensing frequencies is also investigated showing the deterioration in the transceivers performance at lower sensing frequencies. To demonstrate the investigation a TH code length of $N_s = 3$ was used while comparing between sensing the spectrum every T_{sense} and every 2 T_{sense}. Performance deterioration by about 1 dB at BER of 0.001 was observed as the sensing frequency is minimized. Moreover a TH code length of

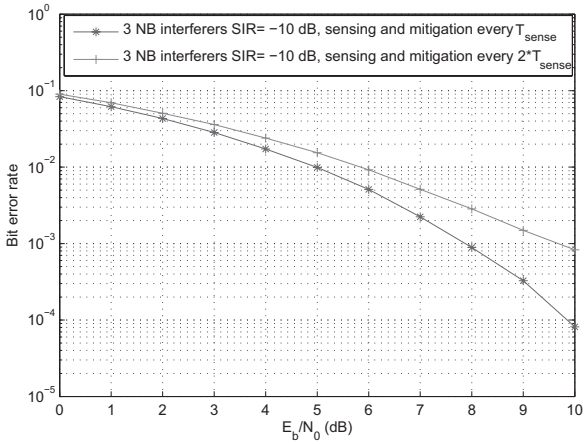

Fig. 22. Normalized transfer function of the matched filter with and without the TH code design in the presence of NB interferer at $f_n = 2.412$ GHz at $N_s = 32$.

$N_s = 8$ was used. Comparing between sensing the spectrum every T_{sense} and every 2 T_{sense}, performance degradation by about 1.5 dB at BER of 0.001 is figured out.

REFERENCES

[1] L. Yang and G. B. Giannakis, "Ultra-wideband communications: an idea whose time has come," *IEEE Signal Process. Mag.*, pp. 26–54, Nov. 2004.

[2] "FCC first report and order: In the matter of revision of part 15 of the commission rule regarding ultra-wideband transmission systems," FCC 02–48, Apr. 2002.

[3] M. Z. Win and R. A. Scholtz, "Impulse radio: How it works," *IEEE Commun. Lett.*, pp. 36–38, vol. 2, no. 2, Feb. 1998.

[4] M. Z. Win and R. A. Scholtz, "Ultra-wide bandwidth time-hopping spread-spectrum impulse radio for wireless multiple-access communications," *IEEE Trans. Commun.*, vol. 48, pp. 679–691, Apr. 2000.

[5] M. A. Rahman, S. Sasaki, J. Zhou, and H. kikuchi, "Error analysis for a hybrid DS/TH impulse radio UWB multiple access system," *IEEE ICU*, (Zurich, Switzerland), Sept. 2005.

[6] S. Gezici *et al.* "Localization via ultra-wideband radios: A look at positioning aspects for future sensor networks," *IEEE Signal Process. Mag.*, pp. 70–84, vol. 22, no. 4, July 2005.

[7] S. Kandeepan and A. Giorgetti: "Cognitive radio techniques: Spectrum sensing, interefrence mitigation and localization," *Artech House*, Oct. 2012.

[8] H. Arslan: "Cognitive radio, software defined radio, and adaptive wireless systems", Springer, 2007.

[9] A. Giorgetti, M. Chiani, and M. Win, "The effect of narrowband interference on wideband wireless communication systems," *IEEE Trans. Commun.*, vol. 53, pp. 2139–2149, Dec. 2005.

[10] M. Chiani and A. Giorgetti, "Coexistence between UWB and narrowband wireless communication systems," *Proc. IEEE*, vol. 97, pp. 231–254, Feb. 2009.

[11] J. Wang and W. T. Tung, "Narrowband interference suppression in time hopping impulse radio ultra wideband communications," *IEEE Trans. Commun.*, vol. 54, pp. 1057–1067, June 2006.

[12] B. Gaffney and A. Fagan, "Adaptive nonlinear narrow band interference rejection in ternary DS-UWB," in *Proc. IEEE ICC*, 2006, pp. 3146–3150.

[13] I. Bergel, E. Fishler, and H. Messer, "Narrowband interference suppression in time-hopping impulse-radio systems," in *Proc. IEEE UWBST*, 2002, pp. 303–307.

[14] N. C. Beaulieu and B. Hu, "On determining a best pulse shape for multiple access ultra-wideband communication systems," *IEEE Trans. Wireless Commun.*, vol. 7, pp. 3589–3596, Sept. 2008.

[15] N. C. Beaulieu and B. Hu, "A pulse design paradigm for ultra-wideband communication systems," *IEEE Trans. Wireless Commun.*, vol. 5, pp. 1274–1278, June 2006.

[16] L. Piazzo and J. Romme, "Spectrum control by means of the TH code in UWB systems," in *Proc. IEEE VTC*, 2003, pp. 1649–1653.

[17] A. Giorgetti, M. Chiani, D. Dardari, R. Piesiewicz, and G. Bruck, "The cognitive radio paradigm for ultra wideband systems: The European project EUWB," in *Proc. IEEE ICUWB*, 2008, pp. 169–172.

[18] A. Giorgetti, "Interference mitigation technique by sequence design in UWB cognitive radio," in *Proc. IEEE CogART*, Nov. 2010, pp. 101–105.

[19] Hua Shao and N. C. Beaulieu, "Direct sequence and time-hopping sequence designs for narrowband interference mitigation in impulse radio UWB systems," *IEEE Trans. Commun.*, vol. 59, pp. 1957–1965, July 2011.

[20] Haykin, "Cognitive radio: Brain-empowered wireless communications," *IEEE J. Sel. Areas Commun.*, vol. 23, pp. 201–220, 2005.

[21] H. Sheng *et al.*, "On the spectral and power requirements for ultra-wideband transmission," in *Proc. IEEE ICC*, vol. 1, May 2003, pp. 738–742.

[22] Cabric, A. Tkachenko, and R. Brodersen, "Spectrum sensing measurements of pilot, energy, and collaborative detection," in *Proc. IEEE Military Commun. Conf.*, Washington, D.C., USA, Oct. 2006, pp. 1–7.

[23] S. Shankar, C. Cordeiro, and K. Challapali, "Spectrum agile radios: Utilization and sensing architectures," in *Proc. IEEE DySPAN*, Baltimore, Maryland, USA, Nov. 2005, pp. 160–169.

[24] Y. Yuan *et al.*, "KNOWS: Cognitive radio networks over white spaces," in *Proc. IEEE DySPAN*, Dublin, Ireland, Apr. 2007, pp. 416–427.

[25] G. Proakis, "Digital communications," McGraw-Hill, 1995.

[26] H. Urkowitz, "Energy detection of unknown deterministic signals," *Proc. IEEE*, vol. 55, pp. 523–531, Apr. 1967.

[27] F. Digham, M. Alouini, and M. Simon, "On the energy detection of unknown signals over fading channels," in *Proc. IEEE ICC*, vol. 5, Seattle, Washington, USA, May 2003, pp. 3575–3579.

[28] Toni. J, "Traffic analysis and design of wireless IP networks," Artech House, Boston 2003.

[29] S. Kandeepan, A. B. Rahim, T. C. Aysal, and Radoslaw Piesiewicz, "Time divisional and time-frequency divisional cooperative spectrum sensing," in *Proc. IEEE/ICST CrownCom*, June 2009.

[30] R. Tandra and A. Sahai. "Fundamental limits on detection in low SNR under noise uncertainty," in *Proc. IEEE WiCOM*, June 2005.

[31] A. Mariani, A. Giorgetti, and M. Chiani, "Effects of noise power estimation on energy detection for cognitive radio applications," *IEEE Trans. Commun.*, vol. 59, no. 12, pp. 3410–3420, Dec. 2011.

Mohamed Essam Khedr received Ph.D. degree from Ottawa University, ECE Department, Canada. He was awarded B.Sc and M.Sc degrees from Arab Academy of Science, Technology Maritime Transport, Collage of Engineering and technology, Egypt. Prof. Khedr research interests are in the fields of wireless communications and networking. He is currently Dean of Student Affairs at Arab Academy of Science, Technology Maritime Transport.

Amr M. Elhelw received Ph.D. degree from Staffordshire University, Faculty of Engineering and technology, UK. He was awarded B.Sc and M.Sc degrees from Arab Academy of Science, Technology Maritime Transport, Collage of Engineering and Technology, Egypt. During his early career he worked as a Researcher and Part Time Lecturer at Staffordshire University. He was granted Gradex 2007 Award for the Best Research Done in 2007 from Staffordshire University. His research work is mainly focused on; telecommunication, digital signal processing, artificial intelligence, pattern recognition, and video and image processing. He is particularly interested in developing new techniques and carrying out high quality research to emphasize real-world applications. He held the university position of quality assurance coordinator. He is currently Director of International Agreements & Cooperation Unit (IACU).

Mohamed Hossam Afifi received his B.S. and M.Sc. degrees in Electrical Engineering from Department of Electronics and Communications, Arab Academy for Science, Technology (AAST), Alexandria, Egypt in 2009 and 2012, respectively. He is currently a Research Assistant at the Department of Electrical and Computer Engineering, Michigan State University (MSU), East Lansing, Michigan, USA. His research interests include wireless communications, signal processing, network security, cryptography, and wireless sensor networks. .